Role of the Interface in the Melt-Rheology Properties of Linear Low-Density Polyethylene/Low-Density Polyethylene Blends: Effect of the Molecular Architecture of the Dispersed Phase

N. Robledo,[1] J. F. Vega,[1] J. Nieto,[2] J. Martínez-Salazar[1]

[1]*Departamento de Física Macromolecular, Instituto de Estructura de la Materia, CSIC, Serrano 113 bis, 28006 Madrid, Spain*
[2]*Dow Chemical Ibérica S.L., Tarragona, Spain*

Received 2 September 2009; accepted 23 May 2010
DOI 10.1002/app.32843
Published online 24 September 2010 in Wiley Online Library (wileyonlinelibrary.com).

ABSTRACT: We studied the melt linear viscoelastic and elongational properties of blends consisting of a Ziegler–Natta linear low-density polyethylene (LLDPE) and different LDPEs. The weight fraction of the LDPE used in the blends was 15%. The linear viscoelastic characterization was performed at different temperatures for all of the blends to determine the thermorheological behavior in the melt state. The blends fulfilled the time–temperature superposition but exhibited a broad linear viscoelastic response, which was further than that expected for miscible blends and even immiscible systems with a sharp interface. A rheological study of the application of the Palierne model revealed that in addition to the droplet shape relaxation, another mechanism was present at lower frequencies. We discuss the results by hypothesizing a strong interaction between the high-molecular-weight linear fraction of the LLDPE matrix and a fraction of molecules of the dispersed phase, which formed a thick interface with its own viscoelastic properties. A clear change in this additional mechanism was observed, depending on the dispersed minor-phase properties, which produced an impact on the processing of the blends, and more precisely, on the values of the melt strength in the melt-spinning experiments. © 2010 Wiley Periodicals, Inc. J Appl Polym Sci 119: 3217–3226, 2011

Key words: blends; immiscibility; interfaces; rheology

INTRODUCTION

Polymer blending is a common and efficient route for obtaining new materials with suitable combinations of processing and end-use properties. However, most polymers are inherently immiscible, even when they have similar monomer chemistry, as occurs in polyolefins. Blends of low-density polyethylene (LDPE) and linear low-density polyethylene (LLDPE) have been extensively studied in recent decades, and a dichotomy of results supporting both miscibility and immiscibility can be found.[1–11] We recently reported that LLDPE-rich blends (with 5–15% LDPE) were immiscible, and the final properties were strongly dependent on the molecular architecture of the LLDPE matrix (Ziegler–Natta or metallocene).[12] In the case of blends of Ziegler–Natta LLDPE with LDPE, an additional contribution in the linear viscoelastic spectrum was found, which was not explained by the assumption of a simple dispersion of LDPE droplets in the LLDPE matrix. This additional contribution was not present when the matrix was a homogeneous LLDPE obtained by means of a single-site catalyst. We suspect that this additional contribution was due to the existence of a thick interphase, presumably formed by a fraction of the longest linear molecules of the LLDPE matrix and the smallest, less branched molecules (rich ethylene sequences) of the LDPE minor phase. This interphase gave rise to a very long relaxation time tail, which could be explained by a viscoelastic model that includes the effect of nonisotropic interfacial effects with a high elastic character. Wagner et al.[9] also reported a singular behavior in this type of blend, which was explained by the assumption a two-phase system: one phase formed by the branched shorter chains of both components and a second phase composed of the longer chains (mostly linear) of both components. More recently, Mieda and Yamaguchi[11] also reported an additional melt-relaxation mechanism in this type of blend. They

Correspondence to: J. F. Vega (imtv477@iem.cfmac.csic.es).
Contract grant sponsor: Dow Chemical Ibérica S. L.
Contract grant sponsor: CICYT; contract grant numbers: MAT2006-0400 and MAT2009-12364.
Contract grant sponsor: CSIC (to N.R. through a 2006 I3P postgraduate fellowship).

TABLE I
Properties of the Pure Materials Used in This Study at $T = 160°C$

Resin	Process	MFI (g/10 min)[a]	M_w (kg/mol)[b]	M_w/M_n[b]	LCB_f[b]	E_{aH} (kcal/mol)	E_{aV} (kcal/mol)	η_0 (kPa·s)	τ_0 (s)	F_{max} (mN)
LLDPE	Solution	1.1	112.4	3.96	–	8.2	0.7	15.3	0.39	9.40
LDPE 1	Autoclave	0.5	254.7	11.1	2.6	17.8	2.9	100.5	153.0	160
LDPE 2	Autoclave	0.9	266.2	12.7	3.1	17.3	2.6	77.4	122.4	154
LDPE 3	Autoclave	1.6	243.7	12.0	3.6	16.6	1.2	44.6	45.3	108
LDPE 4	Autoclave	2.3	239.4	12.0	3.0	15.8	2.0	25.1	18.2	94.8
LDPE 5	Tubular	0.8	89.4	4.91	ND	21.7	3.3	48.7	13.1	65.3

M_w/M_n = polydispersity index (where M_n is the number-average molecular weight); LCB_f = long-chain branching frequency; F_{max} = maximum melt tensile stress; ND = not determined.
[a] Melt index = 190°C, 2.16 kg.
[b] Average values between two and three different runs.

assumed that the behavior observed was not due to phase separation but more likely to entanglement couplings associated with long-chain branching.

In this study, we focused our attention on the effect of the characteristics of the minor phase (LDPE) in the interfacial properties of blends with a Ziegler–Natta LLDPE sample. We studied the thermorheological properties of blends consisting of a LLDPE and different LDPE samples with a variety of melt flow indices (MFIs). The morphology of the various blends was studied by means of the application to the linear viscoelastic results of theoretical models developed for immiscible blends. Also, the processability in the extensional flow in melt-spinning experiments was investigated.

EXPERIMENTAL

The LLDPE sample was a commercial polyethylene-grade Ziegler–Natta LLDPE. This material was mixed with several commercial LDPE samples synthesized from high-pressure radical polymerization processes, both from an autoclave high-pressure polymerization process (LDPE 1–LDPE 4) and a tubular high-pressure polymerization process (LDPE 5). Dow Chemical Ibérica S. L. (Tarragona, Spain) supplied all the materials used in this study. Some of their molecular and physical features are collected in Table I.

The LDPE samples, with a thermal stabilizer, were mixed as the minor phase with 85% of the commercial polyethylene-grade Ziegler–Natta LLDPE. The mixing was performed in a Haake mixer (Karlsruhe, Germany) at a temperature of 180°C for 20 min. The individual pure components also had the same processing history. The sample sheets obtained were compression-molded at 160°C in a Schwabenthan Polystat 200T hot press for 5 min and at a nominal pressure of 150 bar for 10 min and then cooled to room temperature. Sheets of around 1 mm thickness were molded, and disks of suitable dimensions for rheological measurements were obtained.

The shear moduli [storage modulus (G') and loss modulus (G'')] were measured in parallel-plate geometry (diameter = 15 mm) in a stress-controlled Bohlin CVO rheometer (Worcertershire, UK) at 130, 160, and 190°C. The dynamic property determination was carried out within the frequency range 10^{-2}–10^2 rad/s. Deformation was set around 10% or lower, which corresponded to the linear viscoelastic region in all of the pure polymers and blends, as identified through previous amplitude sweeps. The thermal stability of the samples was confirmed by means of time sweeps at low frequencies (0.6–6 rad/s) in the temperature range of study. The data obtained from the frequency sweep tests at different temperatures were shifted at reference temperature (T_R = 160°C) with the time–temperature superposition principle (TTSP).

The extensional properties of the polymers in the melt-spinning experiments were measured at a temperature of 160°C with a CEAST Rheoscope 1000 (Pianezza TO, Italy) capillary rheometer equipped with a specific set of rotating wheels and a tension detector (stretching unit). The capillary was a circular cross section (diameter = 1 mm) with a length/diameter ratio of 20. The length of the spin line was constant and equal to 200 mm, and the die exit velocity (v_0) was 2 mm/min and remained constant during the experiments. The force required for the extension of the polymer extrudates (F) was evaluated by the steep increase of the rotating wheels' draw-down velocity, up to the breakup of the filaments. Under these conditions, it seemed reasonable to assume that the cooling of the filament during the experiment was moderate and that the conditions were quasi-isothermal.

The extensional stress (σ_{11}) was determined with the following expression:

$$\sigma_{11} = \frac{F}{A_0} V \tag{1}$$

where A_0 is the cross section of the die ($A_0 = \pi R_C^2$) and V is the draw ratio ($V = v_1/v_0$, where v_1 is the take-up velocity at the rotor).

RESULTS AND DISCUSSION

Rheology of the pure polymers and blends

Figure 1(a) depicts the complex viscosity [$\eta^*(\omega)$] obtained for some of the pure polymers listed in Table I as a function of the angular frequency at T_R = 160°C after application of the TTSP. The data obtained at different temperatures were shifted at T_R with the method developed by Mavridis and Shroff.[13] This methodology allowed us to obtain the temperature shift factors [horizontal shift factor (a_T) and vertical shift factor(b_T)] defined for the frequency and complex modulus, respectively. a_T can be interpreted in terms of the horizontal flow activation energy (E_{aH}) values. Similarly, b_T is defined in terms of a vertical flow activation energy (E_{aV}). The application of b_T is necessary in thermorheological complex systems of long-chain branched polyolefins and blends of linear and branched molecular species.[13] All of the LDPE samples and LLDPE/LDPE blends studied here were thermorheologically complex, and the necessary b_T was applied for TTSP.

The most commonly used equation to describe the thermal dependence of the rheological properties of polymeric systems is the William–Landel–Ferry (WLF) expression.[14] This expression is generally applicable in the temperature range between the glass-transition temperature (T_g), and T_g + 100°C. For higher temperatures, it can be closely approximated by an Arrhenius-type equation:

$$a_T = \exp\left(\frac{E_{aH}}{R}\left(\frac{1}{T}-\frac{1}{T_R}\right)\right), b_T = \exp\left(\frac{E_{aV}}{R}\left(\frac{1}{T}-\frac{1}{T_R}\right)\right) \quad (2)$$

where R is the gas constant and T is the experimental temperature. From the values of a_T and b_T and with these expressions, it is possible calculate the activation energy values. The values for the pure materials studied are listed in Table I. LLDPE presented no signs of thermorheological complexity ($b_T \approx 1$), with E_{aV} being very low, close to zero. However, as expected, the LDPE samples presented thermorheological complexity, which means that the E_{aV} values were nonzero (2–3 kcal/mol). Moreover, these samples showed E_{aH} values higher than the LLDPE sample, around 15.0–20.0 kcal/mol, a typical feature of long-chain-branched polyolefins. This complex behavior was attributed to the different relaxation mechanisms of the branched chains in an entangled environment compared to linear macromolecules. On the other hand, comparing the tubular LDPE 5 and the autoclave LDPE 2 samples with similar MFIs, we observed that the former showed a higher viscosity at lower frequencies and a lower E_{aH} value. Other studies concerning physical properties of LDPE samples have shown that these differences are likely due to a different branched structure in the tubular and autoclave LDPE samples.[15–20] In the case of LLDPE, the viscosity curve approached the Newtonian viscosity (η_0) at low frequencies. Notwithstanding, it exhibited a certain degree of shear thinning, as expected for a polydisperse system. In comparison, the LDPE samples showed a stronger shear thinning behavior; the viscosity was much more dependent on the oscillation frequency than that of LLDPE, a behavior attributed to both the broad molecular weight distribution and the presence of long-chain branches.

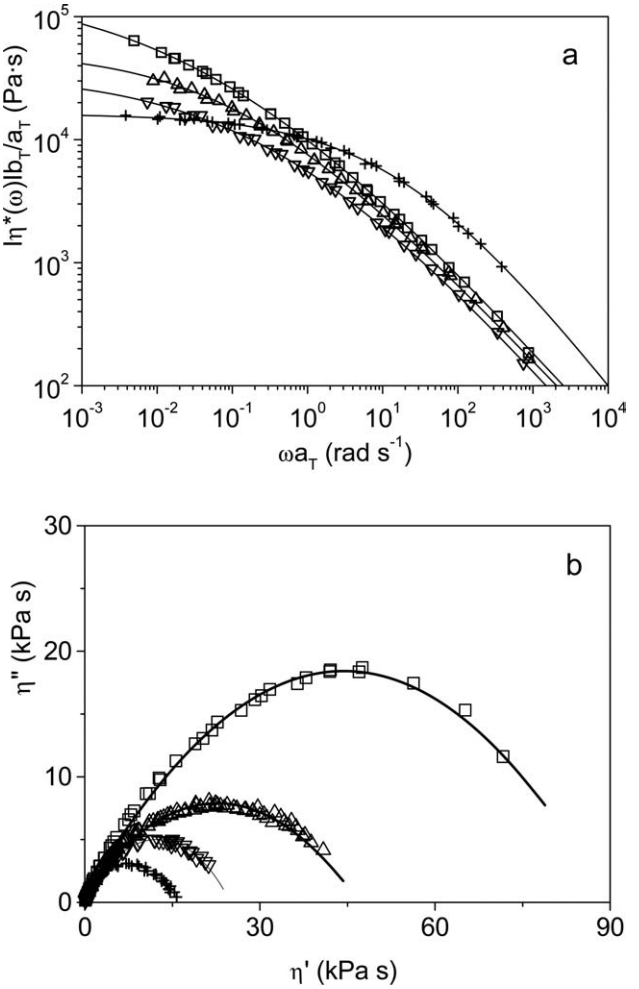

Figure 1 (a) $\eta^*(\omega)$ curves and (b) Cole–Cole plots for some of the pure samples superposed to a T_R of 160°C: (+) LLDPE, (□) LDPE 1, (△) LDPE 3, and (▽) LDPE 4.

Lanfray and Marin[21] reported a simple method for analyzing the dynamic rheological results of molten entangled polymers and obtaining η_0. They showed the suitability of the Cole–Cole representation of real and imaginary parts of the complex viscosity [$\eta^*(i\omega)$]. The representation of the out-of-phase component of complex viscosity, η'', versus the dynamic

TABLE II
Properties of the LLDPE/LDPE (15% LDPE) Blends Studied at T_R = 160°C

Blend	E_{aH} (kcal/mol)	E_{aV} (kcal/mol)	η_0 (kPa·s)	α/R (kN/m)	β''/R (kN/m)	τ_α (s)[a]	τ_α (s)[b]	τ_β (s)[a]	τ_β (s)[b]	F_{max} (mN)	K
LLDPE/LDPE 1	10.0	1.0	30.0	1.5	0.40	11.5	15.3	220	290	65.9	3.8
LLDPE/LDPE 2	9.3	0.8	27.7	2.3	0.40	8.1	9.9	180	230	56.8	3.2
LLDPE/LDPE 3	9.0	1.5	22.7	4.2	0.40	5.5	5.4	130	200	45.8	3.2
LLDPE/LDPE 4	9.4	0.4	20.7	8.0	0.40	4.1	2.9	97	115	42.4	2.7
LLDPE/LDPE 5	10.1	0.4	25.6	3.5	0.60	6.6	6.5	78	106	37.5	1.7

α/R and β''/R = hydrodynamic features of the blends from the Palierne model; τ_α and τ_β = corresponding relaxation times associated with the terminal response of the blends; K = ratio of the maximum tensile stress of the blends to the corresponding to the dispersed LDPE sample.
[a] Obtained from empirical splitting of the τ_i distribution spectra.
[b] Obtained from eqs. (9) and (10).

viscosity, η', and the real axis; λ_0, a characteristic relaxation time that corresponds to the reciprocal frequency at the maximum of μ'', ω_{max}; and β, which is the dispersion parameter and is defined as the angle between the diameter through the origin of the circular arc and the real axis:

$$\eta^*(i\omega) = \frac{\eta_0}{1 + (i\omega\lambda_0)^{1-\beta}} \quad (3)$$

The Cole–Cole model provides an accurate fit to the experimental data over the usual frequency range with only these three parameters for many flexible polymers. The experimental data of the pure samples examined in this study fit to obtain η_0 from eq. (3) are presented in Figure 1(b). The values of η_0 for the pure samples at 160°C are listed in Table I.

Concerning the blends, the TTSP seemed to properly work in all cases. In the case of polymer blends, the fulfillment of the TTSP cannot be considered a good test of miscibility.[22] The addition of LDPE to LLDPE causes an increase in the E_{aH} values, with E_{aV} remaining lower than 1 kcal/mol (see Table II). This is a common behavior in LLDPE/LDPE blends. In Figure 2 are shown the Cole–Cole plots of the pure materials and some of the blends studied. It was not possible to distinguish between different relaxation mechanisms corresponding to the different molecular species, as a unique broad response proceeded. Also, some of the blends showed η_0 close to or higher than those corresponding to both pure samples (cf. the values in Tables I and II). This result involved a shifted viscoelastic response to lower frequencies or higher relaxation time values than those corresponding to the average molecular species of both blends' components. This strong deviation from the expected behavior indicated the existence of additional relaxation mechanisms, as reported in nonhomogeneous blends.[23–26]

Analysis of the linear viscoelastic response of the blends

Application of the Palierne model to the linear rheological response

The morphology of nonhomogeneous polymer blends likely consists of droplets of the minor phase immersed into the major phase (the matrix). The shape, size, and interactions of these droplets with the matrix strongly affect the linear viscoelasticity, processing, and final properties of the products. The study of the morphology of the polyolefin blends is very complex, as a poor contrast between the phases is found. In this case, dynamic small-amplitude oscillatory measurements were of interest, as the linear viscoelastic response was very sensitive to the morphological aspects of the blends. The study of the melt-state dynamic shear features is very useful, as

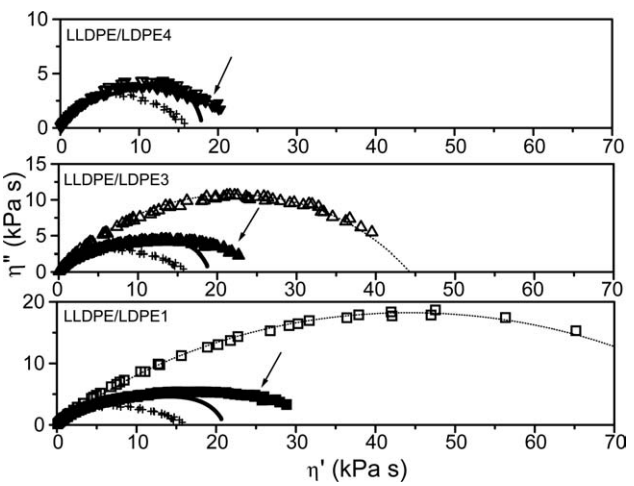

Figure 2 Cole–Cole plots of $\eta^*(\omega)$ at a T_R of 160°C for the pure polymers [(+) LLDPE, (□) LDPE 1, (△) LDPE 3, and (▽) LDPE 4] and their blends with LLDPE (solid symbols). The solid lines correspond to the results of the application of the Palierne model (see the text).

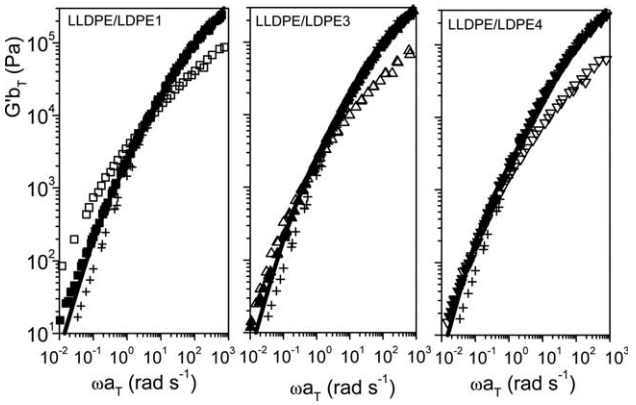

Figure 3 G' superposed to a T_R of 160°C for the pure samples and some of the blends (see Fig. 2 for an explanation of the symbols).

they can be related to the blend morphology by means of the use of the Palierne model, which is widely used to estimate the average radius of the dispersed phase and/or the characteristic interfacial tension (α) between the components.[23] This model predicts the existence of an additional slow relaxation mechanism (low frequencies), which was interpreted as the dispersed droplet deformation process. The model describes de complex shear modulus of the blend, $G^*(\omega)$, in terms of the properties of each phase, the complex moduli of the matrix and dispersed phase, $G_m^*(\omega)$ and $G_d^*(\omega)$, respectively, by means of the following expression:

$$G^*(\omega) = G_m^*(\omega)\frac{1 + 3\sum_i \phi_i H_i(\omega)}{1 - 2\sum_i \phi_i H_i(\omega)} \tag{4}$$

where $H_i(\omega)$ is a function that contains materials and blend features and is determined as follows:

$$H_i(\omega) = \frac{4(\frac{\alpha}{R})[2G_m^*(\omega) + 5G_d^*(\omega)] + [G_d^*(\omega) - G_m^*(\omega)][16G_m^*(\omega) + 19G_d^*(\omega)]}{40(\frac{\alpha}{R})[G_m^*(\omega) + G_d^*(\omega)] + [2G_d^*(\omega) + 3G_m^*(\omega)][16G_m^*(\omega) + 19G_d^*(\omega)]} \tag{5}$$

These equations predict that the enhancement of viscoelastic functions due to the presence of a dispersed phase mainly depends on α between the phases, the particle radius (R), and the volume fraction (ϕ).

In Figures 2 and 3 are shown the results obtained upon the application of the model to the linear viscoelastic functions of the different blends studied over a wide range of frequencies (5 decades). The values of α used varied between 1.0×10^3 and 10×10^3 N/m^2, in a range repeatedly reported in the literature for this type of blend.[27–31] The model given by the simple formulation of eqs. (4) and (5) was not able to explain the experimental results obtained in the whole range of frequencies. In a previous work, we already revealed that the application of this model for LLDPE/LDPE blends did not explain the experimental shear moduli measured, as the broad relaxation response could not be described only as a consequence of the shape relaxation mechanism of the dispersed LDPE droplets. A change in the parameter α/R did not improve the prediction.[12] An additional relaxation mechanism should be postulated to explain the broadening of the melt mechanical relaxation. The matrix was a Ziegler–Natta copolymer, characterized by a complex molecular architecture. This LLDPE was actually a mixture of molecules in a continuous range from low-molecular-weight branched species to high-molecular-weight linear species. This linear high-molecular-weight tail possessed the highest relaxation time of the distribution. Moreover, the relaxation time values of this tail spread to the same time region as the average relaxation time (τ_0) of the dispersed LDPE droplets. It is documented in the literature that linear polyethylene (high-density polyethylene) is miscible with LDPE in a whole range of compositions in blends prepared under similar conditions to those used in this study.[5,6] Then, we expected some kind of interaction between the linear species from LLDPE and the lowest molecular weight species from LDPE samples because both had very high relaxation time values.[12] The morphological picture proposed for the LLDPE/LDPE blends here was similar to that proposed by Wagner et al.[9] These authors suggested a two-phase system composed by one phase with the branched shortest chains of both LLDPE and LDPE polymers and another phase with the longest chains of both components. Other authors have suggested the existence of a third phase in these type of blends composed of chains from both the matrix and the dispersed phase with the ability to cocrystallize, that is, high weight-average molecular weight (M_w) linear chains from LLDPE with high-M_w branched chains from LDPE.[10]

It is important for further discussions to take into account that the interfacial properties between LLDPE and LDPE in our blends could be eventually modified and also should have had their own viscoelastic properties. In addition to the isotropic α, such an interface is characterized by an interfacial elasticity.[30] The extended model of Palierne[32] has been proven to adequately describe the linear viscoelastic

data of blends with strong interfacial interactions.[33–38] In this study, different dispersed phases were used in the blends, and so, we expected systematic changes in the interfacial component. The systematic changes in the linear viscoelastic response are shown in Figure 3 for G'. As clearly shown, as MFI of the LDPE minor phase increased, the values of G' of the blends at low frequencies were closest to that shown by the pure LDPE phase at low frequencies.

Viscoelastic properties of the interface

The weighted relaxation spectrum [$H(\tau)$] is very useful for studying the additional relaxation mechanisms associated with the presence of dispersed viscoelastic droplets in a matrix.[10,25,26,30,39] The relationship between $H(\tau)$ and the shear dynamic moduli, G' and G'', can be expressed by[14]

$$G'(\omega) = \sum_i h_i \frac{\omega^2 \tau_i^2}{1 + \omega^2 \tau_i^2} \tag{6}$$

where (h_i,τ_i) represents the discrete Maxwell relaxation time distribution.

$$G''(\omega) = \sum_i h_i \frac{\omega \tau_i}{1 + \omega^2 \tau_i^2} \tag{7}$$

We applied a nonlinear regression fitting procedure to obtain $H(\tau)$ from the dynamic mechanical data. The τ_i's were fixed at equally spaced intervals; τ_i/τ_{i-1} was a constant (with the minimum relaxation time defined as $\tau_{min} = 1/\omega_{max}$, being ω_{max} the maximum experimental frequency). The number of data points per decade was specified to be 1.5 to minimize ill-posed problems. With these conditions, the relaxation time spectrum was directly related to the experimental frequency range. Then, we could easily obtain the related continuous function, $H(\tau)$ from[40]

$$h_i(\tau_i) = H(\tau)\Delta \ln \tau \approx H(\tau) \ln\left(\frac{\tau i}{\tau_{i-1}}\right) \tag{8}$$

Figure 4(a) shows the relaxation time spectrum for the LLDPE/LDPE 5 blend. The characteristic τ_0 values were revealed as maxima, which could be easily analyzed quantitatively. The spectrum curve for the LLDPE/LDPE 5 blend had a single peak that comprised τ_0 values of both the LLDPE and LDPE pure components. We observed that the experimental relaxation (solid symbols) was broader than that obtained by the modeling of the viscoelastic response by means of the Palierne model (with α = 1.0–10 $\times$ 10^3 N/m^2), which gave rise to two relaxation mechanisms, the bulk blend relaxation and the shape droplet relaxation (α). The relaxation time distribution of this blend showed a longer tail than that

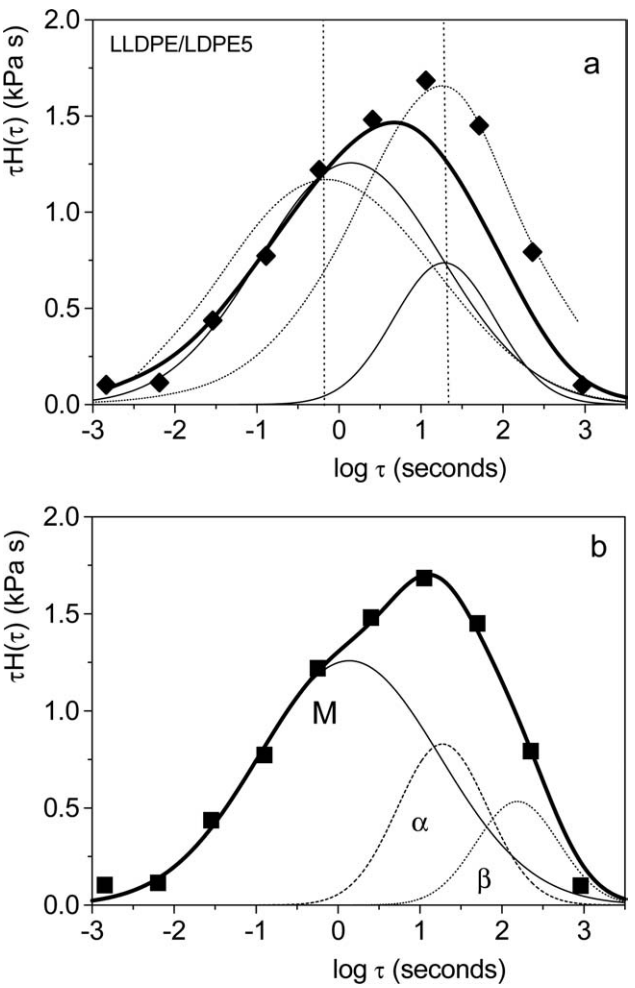

Figure 4 (a) Weighted relaxation time spectra of (+) pure LLDPE and (◇) pure LDPE 5 (dotted lines) and (◆) the LLDPE/LDPE 5 blend at a T_R of 160°C. The solid lines corresponds to the main relaxation and shape deformation relaxation predicted by the Palierne model (thick, solid line). (b) Identification of the different relaxation mechanisms by empirical Gaussian splitting of the weighted $H(\tau)$ for the LLDPE/LDPE 5 blend.

corresponding to the pure LDPE sample, which represented around 15% of the total response. This was a clear indication of strongly cooperative or overlapped mechanisms in the whole time domain, as was also suggested by the unique temperature dependence of the viscoelastic properties in the time range explored. An extra contribution should be included to explain the whole $H(\tau)$, as shown in Figure 4(b). This additional relaxation appeared at the longest relaxation time region, and it could be interpreted as the interfacial contribution (β). Molecular interaction between different fractions of the mixed samples would promote the accumulation of certain molecular species, preferentially at the interface and causing changes in the particle size and an improved adhesion between the blend components. From a microscopic point of view, the presence of

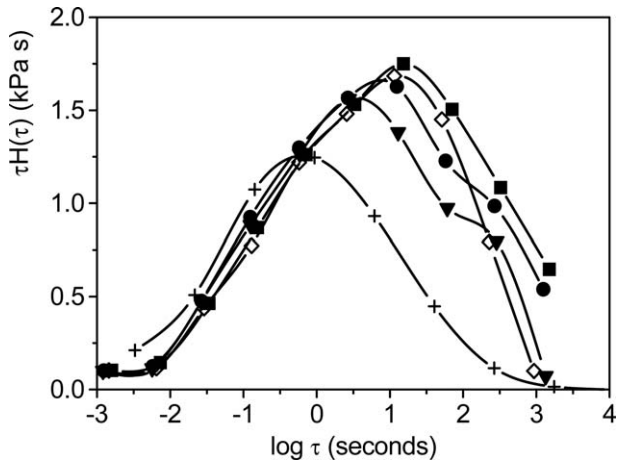

Figure 5 Weighted relaxation spectra of (+) pure LLDPE, (■) LLDPE/LDPE 1, (●) LLDPE/LDPE 2, (▼) LLDPE/LDPE 4, and (◇) LLDPE/LDPE5 at a T_R of 160°C.

these molecular species enlarged the thickness of the interface. This interface contributed with an additional relaxation process characterized with a very large interfacial relaxation time (τ_β). Moreover, the properties of this interface should have now been strongly dependent on the nature, molecular weight, and amounts of the involved species.

If both LLDPE and LDPE species are involved in the interface, a systematic change in the LDPE type dispersed phase should also promote different interfacial contributions at a given composition. The differences found in the blends studied are shown in Figure 5. A strong effect of the LDPE phase was clearly identified, as a systematic shift of the relaxation time distribution was obtained as the MFI of the LDPE changed. Decreases in the strength and in the values of the characteristic time of the β relaxation as relaxation time of the dispersed LDPE phase decreases were clear from the results. The blends with the LDPE 2 and LDPE 5 samples were especially interesting. Both LDPE samples had similar MFI but likely a different branched structure (because of the different polymerization process, as indicated in the preceding lines). The relaxation time distributions of the blends were then totally different; this suggested different interfacial properties. The isolated β relaxation (assumed as a Gaussian contribution, additional to the Palierne response) for all of the blends studied is plotted in Figure 6. From these results, we extracted the values of the strength (H_β) and τ_β of the additional relaxation, as listed in Table II. Both viscoelastic features nicely scaled with MFI of the LDPE minor phase, and then, it was a process that could be tailored by a change in this component. Moreover, the characteristic values of τ_β, defined at the maximum of the relaxation, were higher than the corresponding averages to both the pure LLDPE matrix and the LDPE dispersed phases (see Table I).

We applied the Palierne model modified by Jacobs et al.,[32] which considers an additional term to the shape deformation of the droplets to account for the viscoelastic properties of the interface. This approach considers an interfacial dilatation modulus ($\beta' = 0$) and an interfacial shear modulus (β''), independent of the frequency (purely elastic interface). As pointed out by these authors, this approach requires two conditions: first, the existence of an additional relaxation mechanism in addition to the shape relaxation of the droplets, and, second, the η_0 values of the blends must only depend on the amount of dispersed phase and not on the interfacial nature. Considering all of the above, Van Hemelrijck et al.[36] found the corresponding expression for G' with only two parameters α/R and β''/R. The fits of the experimental data of G' and η'' to the Palierne model with the parameters β''/R and α/R listed in Table II are shown in Figure 7 for the LLDPE/LDPE blends studied. From these fits, the characteristic relaxation mechanism assigned to both the shape deformation time (τ_α) and to the response of the interface (τ_β) were deduced. We made use of the equations for the characteristic relaxation time values on the basis of the extended Palierne model derived by Jacobs et al.[32] We could simplify these equations in our case, considering that $\phi < 1$ and $\beta''/\alpha \ll 1$. In this specific case, the characteristic τ_α and τ_β were obtained as[35]

$$\tau_\alpha = \frac{\eta_m R}{\alpha} f(p) \tag{9}$$

$$\tau_\beta = \frac{\eta_m (1+p) R}{\beta} \tag{10}$$

where η_m is the viscosity of the matrix, p is the ratio between the viscosity of the dispersed phase and

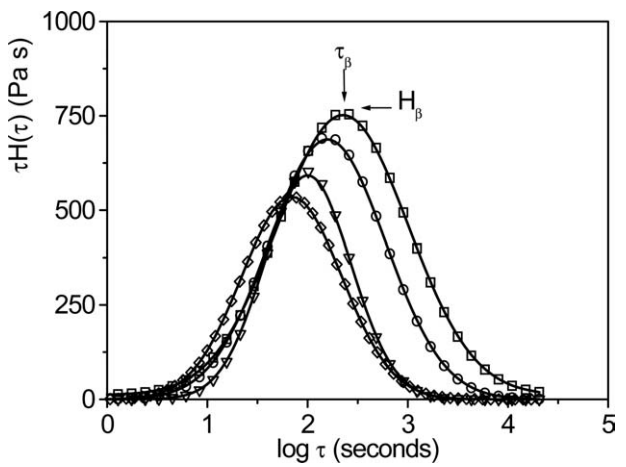

Figure 6 β relaxation contribution obtained from empirical Gaussian splitting of the weighted relaxation time distributions of the blends studied at 160°C: (□) LLDPE/LDPE 1, (○) LLDPE/LDPE 2, (▽) LLDPE/LDPE 4, and (◇) LLDPE/LDPE 5.

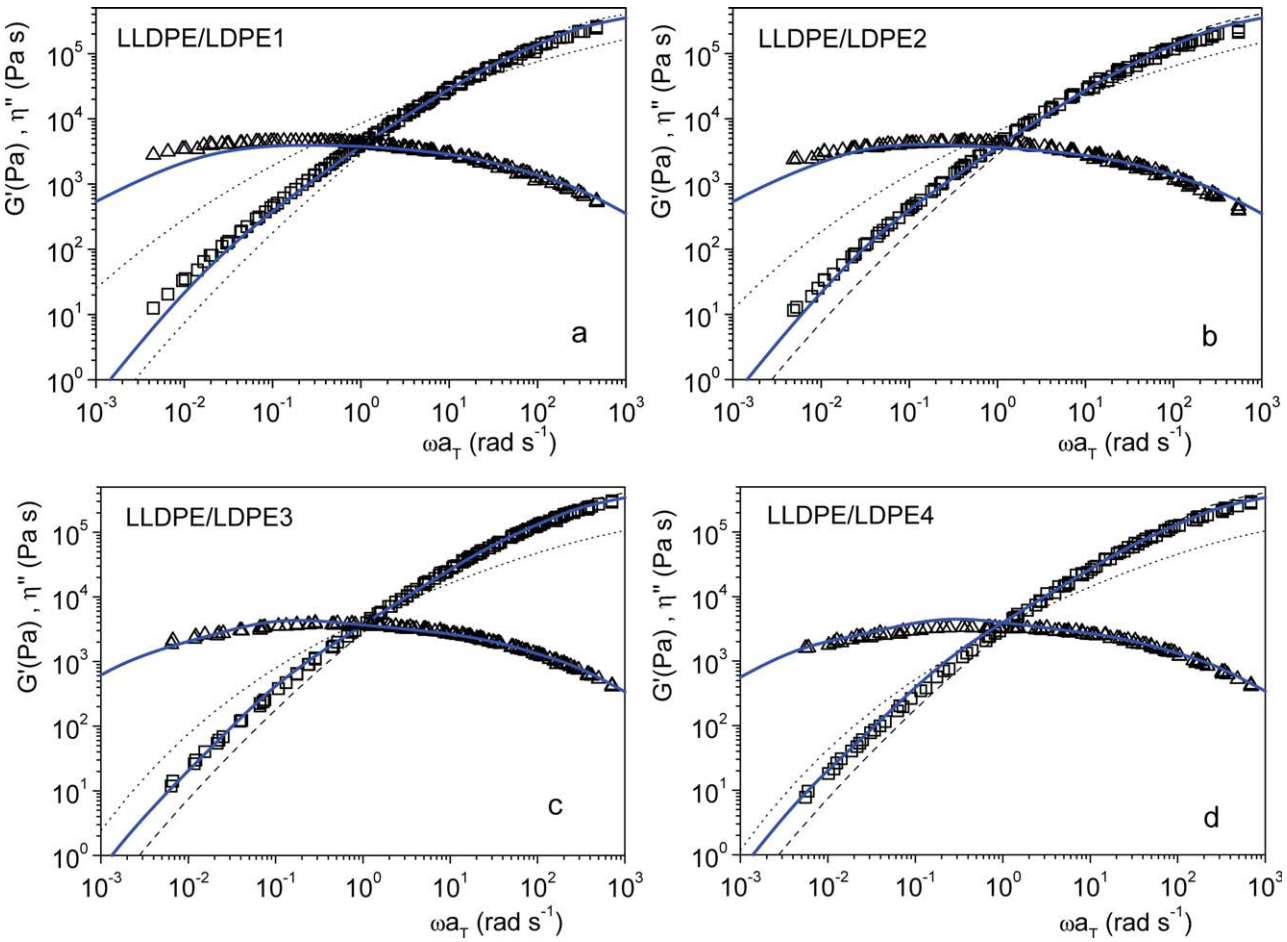

Figure 7 Application of the Palierne model with an additional term for the viscoelastic response of the interface for different values of α/R and β''/R to (□) G' and (△) η'' in the LLDPE/LDPE blends at 160°C: (a) LLDPE/LDPE 1, (b) LLDPE/LDPE 2, (c) LLDPE/LDPE 3, and (d) LLDPE/LDPE 4. Solid lines are the results of the applied model. Dashed lines (LLDPE) and dotted lines (LDPE) are the results of G' for the pure materials. [Color figure can be viewed in the online issue, which is available at wileyonlinelibrary.com.]

that of the matrix, and $f(p)$ is a function that accounts for a weak influence of the viscosity ratio, which varies between 1 and 2 (we considered an average value of 1.5 in our case). The calculated values of τ_α and τ_β are listed in Table II. The calculated relaxation time values of both the α and β relaxations were in good agreement with the obtained results of the empirical separation methodology applied for the blends, as discussed in the preceding lines, as we observed in the comparison made as a function of the values of η_0 of the dispersed phase in Figure 8.

The model was able to capture the characteristic broad linear viscoelastic response, but it was more precise for those blends with the lower values of η_0 (LDPE 3 to LDPE 4, see Fig. 7(c,d)]. In these cases, the η_0 values were practically unaltered by the nature of the second component of the blend, which within the measurements uncertainty was around the theoretical value expected by the Palierne model. The model was not able to completely explain the

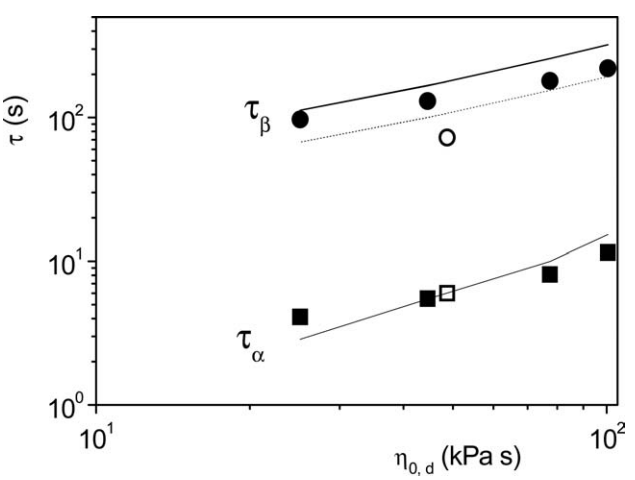

Figure 8 Characteristic relaxation time values: (■) τ_α and (●) τ_β obtained from Gaussian splitting and from fitting to the Palierne model (the solid lines are for $\beta''/R = 0.4$ kN/m^2 and the dotted line is for $\beta''/R = 0.60$ kN/m^2) versus η_0 of the dispersed phase at 160°C for all of the studied blends. The open symbols correspond to the results obtained for the LLDPE/LDPE 5 blend.

response of the blends with LDPE 1 and LDPE 2 dispersed phases [Figs. 7(a,b)], which were characterized by higher values of η_0. These results suggest a complex picture, probably due to the different nature of the molecules at the interface in each of the blends. In a recent study, the additional interfacial response was identified with the Gibbs elasticity as an intrinsic property of the interface, which was the key point for explaining the scaling of the relaxation time values with interfacial properties.[35] In this context, the parameter that actually controlled τ_β was $3M_I\phi/N_a\rho_I\phi_I$ (where N_a is the Avogadro's number, M_I is the molecular weight of the interfacial component, ρ_I is its concentration, and ϕ_I is its volume fraction) or, in other words, the volume occupied by a molecule located at the interface. This treatment explained the increased relaxation time values as the molecular weight of the interfacial molecules increased. If the interface was formed in our blends by both the LLDPE matrix and the different LDPE dispersed components, it seemed reasonable to assume that the increase observed in τ_β was due to the increased molecular size of the LDPE molecular species, as shown in Tables I and II. With these results, one could anticipate a higher stability of the dispersed phase to mechanical deformation in the blends with LDPE with the highest values of dispersed phase η_0 or τ_0 (or lower MFI), and then, the droplets would not easily break upon strong deformations, in contrast to the behavior observed in unstabilized immiscible blends.[36] In the case of the LLDPE/LDPE 5 blend (with the tubular LDPE), a small deviation was observed. This blend had the smaller τ_β contribution, a result probably related to the also smaller value of τ_0 in the pure dispersed phase (LDPE 5) with respect to the autoclave LDPE family (LDPE 1–LDPE 4), as shown in Table I. This was likely due to the different molecular architecture of the tubular LDPE 5 sample. Anyway, the presence of the β contribution ascribed to the interfacial elasticity in these blends may have played an important role not only in the melt-state processing operations but also in the final microstructure and properties (mechanical, optical, etc.) of the finished products, such as films.

Elongational properties: Melt spinning

The load (F) versus V curves measured for the various materials and blends by the melt-spinning tests performed under the aforementioned testing conditions are reported in Figure 8(a,b). V is defined as $V = v_1/v_0$, where v_1 is the stretching velocity at the wheels, which was steadily increased, and v_0 is the die extrusion velocity, which was kept constant during the whole duration of the experiment. Figure 9(a) shows the tensile force for the pure components

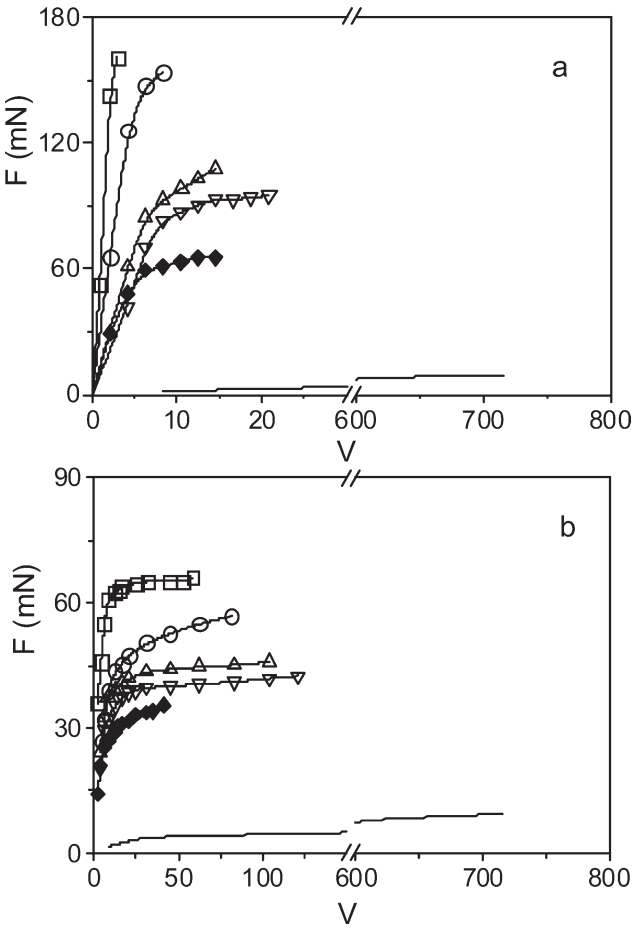

Figure 9 Tensile force versus the drawdown velocity ratio at 160°C for (a) the pure polymers [(—) LLDPE, (□) LDPE 1, (○) LDPE 2, (△) LDPE 3, (▽) LDPE 4, and (◆) LDPE 5] and (b) the LLDPE/LDPE blends (the symbols correspond to the LDPE used in the blend).

as a function of the draw-down ratio. The figure clearly shows the expected difference between the LDPE and LDPE samples. The draw-down force values obtained for the LDPE samples (160–65.3 mN from LDPE 1 to LDPE 5) were higher than that of the LLDPE sample (9.40 mN). This difference was attributed to the differences in the relaxation time distributions and the molecular architecture of the samples. Moreover, in the LDPE samples, there existed a clear increase in the melt strength as the MFI decreased, with the exception of sample LDPE 5, which as it has been indicated in previous lines, likely possessed a different molecular architecture than the rest of the LDPE samples. As it is well known,[41] the presence of long-chain branching and a broader molar mass distributions causes a higher degree of strain hardening in elongation and, as a result, a higher tensile force in melt-spinning experiments.

Figure 9(b) shows the tensile force versus the draw-down velocity ratio measured for the LLDPE/

LDPE blends studied. As clearly shown in this figure, the presence of LDPE induced an increase in the force exhibited by the material in resisting extension at a prescribed V, with respect to neat LLDPE. The maximum tensile force values at the break of the filament were higher than that the corresponding to the pure LLDPE sample in all cases, with values varying between 65.9 mN for the LLDPE/LDPE 1 blend to 37.5 mN for LLDPE/LDPE 5. Furthermore, these values were also above those obtained by the additive rule applied to the corresponding values of the pure components. Moreover, there seemed to exist a correlation between the increase observed in the maximum extensional stress, σ_{11max} obtained from eq. (1) for the blends and the interfacial properties, as the stronger increments given by K in Table II, with $K = \sigma_{11max}(\text{blend})/\sigma_{11max}(\text{LDPE})$, were seen in those blends with a more important contribution of the interfacial component to the linear viscoelastic response.

CONCLUSIONS

We investigated the influence of different LDPE dispersed phases in the linear viscoelastic behavior and elongation in the melt of LLDPE/LDPE blends. The simplified model of Palierne was not efficient in describing the complex relaxation observed in the blends, and an additional relaxation mechanism had to be considered. From this study, it was clear that the LDPE type had a strong effect on this additional mechanism, probably because of the differences in the interfacial properties. The application of the extended model of Palierne identified the additional mechanism with the elastic properties of the interface by means of the introduction of β''. This parameter, together with α and the intrinsic viscoelastic properties of the pure components, explained both qualitatively and quantitatively the very broad τ_i distribution of the blends. The trend observed suggests that those LDPE samples with the highest η_0 (lowest MFI) values induced more elastic interfaces, with characteristically higher relaxation time values. Small differences were found for the blend with the tubular LDPE, which suggested an effect of the different molecular architecture in this case. The presence of the contribution attributed to the interfacial elasticity played an important role in the melt-state processing operations. Strong positive deviations of the maximum tensile stress were found in the melt-spinning experiments. These deviations were more pronounced in those blends with the presumed strongest interfaces.

References

1. Utracki, L. A.; Schlund, B. Polym Eng Sci 1987, 27, 1512.
2. Schlund, B.; Utracki, L. A. Polym Eng Sci 1987, 27, 1523.
3. Cho, K. C.; Lee, B. H.; Hwang, K. M.; Lee, H. S.; Choe, S. J. Polym Eng Sci 1998, 38, 1969.
4. Yamaguchi, M.; Abe, S. J Appl Polym Sci 1999, 74, 3153.
5. Groves, D. J., McLeish, T. C. B.; Chohan, R. K.; Koates, P. D. Rheol Acta 1996, 35, 481.
6. Lee, H. S.; Denn, M. M. Polym Eng Sci 2000, 40, 1132.
7. Peón, J.; Domínguez, C.; Vega, J. F.; Aroca, M.; Martínez-Salazar, J. J Mater Sci 2003, 38, 4757.
8. Hussein, I. A.; Williams, M. C. Rheol Acta 2004, 43, 602.
9. Wagner, M. H.; Kheirandish, S.; Yamaguchi, M. Rheol Acta 2004, 44, 198.
10. Delgadillo-Velázquez, O.; Hatzikiriakos, S. G.; Sentmanat, M. Rheol Acta 2008, 47, 19.
11. Mieda, N.; Yamaguchi, M. Adv Polym Technol 2007, 26, 173.
12. Robledo, N.; Vega, J. F.; Nieto, J.; Martínez-Salazar, J. J Appl Polym Sci 2009, 114, 420.
13. Mavridis, H.; Shroff, R. N. Polym Eng Sci 1992, 32, 1778.
14. Ferry, J. D. Viscoelastic Properties of Polymers, 3rd ed.; Wiley: New York, 1980.
15. Graessley, W. W.; Raju, V. R. J Polym Sci Polym Symp 1984, 71, 77.
16. Kuhn, R.; Kromer, H. Mikrochim Acta 1991, 104, 225.
17. Scholte, T. G.; Meijerink, N. L. J. British Polym J 1977, 9, 133.
18. Kuhn, R.; Kromer, H. Col Polym Sci 1982, 260, 1083.
19. Tackx, P.; Tacx, J. C. J. F. Polymer 1998, 39, 3109.
20. Yamaguchi, M.; Takahashi, M. Polymer 2001, 42, 8663.
21. Lanfray, Y.; Marin, G. Rheol Acta 1990, 29, 390.
22. van Gurp, M.; Palmen, J. Rheol Bull 1998, 67, 5.
23. Palierne, J. F. Rheol Acta 1990, 29, 204.
24. Gramespacher, H.; Meissner, J. J Rheol 1992, 36, 1127.
25. Lacroix, C.; Aressy, M.; Carreau, P. J. Rheol Acta 1997, 36, 416.
26. Yu, W.; Bousmina, M.; Zhou, C. X. J Non-Newt Fluid Mech 2006, 133, 57.
27. Hussein, I. A.; Williams, M. C. Polym Eng Sci 2001, 41, 696.
28. Hussein, I. A.; Hameed, T.; Sharkh, B. F. A.; Mezghani, K. Polymer 2003, 44, 4665.
29. Peón, J.; Aguilar, M.; Vega, J. F.; del Amo, B.; Martinez-Salazar, J. Polymer 2003, 44, 1589.
30. Fang, Y. L.; Carreau, P. J.; Lafleur, P. G. Polym Eng Sci 2005, 45, 1254.
31. Peón, J.; Vega, J. F.; Aroca, M.; Martínez-Salazar, J. J Mater Sci 2006, 41, 4814.
32. Jacobs, U.; Fahrlander, M.; Winterhalter, J.; Friedrich, C. J Rheol 1999, 43, 1495.
33. Riemann, R. E.; Cantow, H. J.; Friedrich, C. Polym Bull 1996, 36, 637.
34. Riemann, R. E.; Cantow, H. J.; Friedrich, C. Macromolecules 1997, 30, 5476.
35. Friedrich, C.; Antonov, Y. Y. Macromolecules 2007, 40, 1283.
36. Van Hemelrijck, E.; Van Puyvelde, P.; Velankar, S.; Macosko, C. W.; Moldenaers, P. J Rheol 2004, 48, 143.
37. Huo, Y. L.; Groeninckx, G.; Moldenaers, P. Rheol Acta 2007, 46, 507.
38. Yee, M.; Calvao, P. S.; Demarquette, N. R. Rheol Acta 2007, 46, 653.
39. Gramespacher, H.; Meissner, J. Theor Appl Rheol 1992, 1–2, 354.
40. Kraft, M.; Meissner, J.; Kaschta, J. Macromolecules 1999, 32, 751.
41. Wagner, M. H.; Schulze, V.; Gottfert, A. Polym Eng Sci 1996, 36, 925.